

## COMPUTER SIMULATION OF HARD-CORE MODELS FOR LIQUID CRYSTALS \*

D. FRENKEL<sup>1</sup>

*Fysisch Laboratorium, Rijksuniversiteit Utrecht, P.O. Box 80000, 3508 TA Utrecht, The Netherlands*

A review is presented of computer simulations of liquid crystal systems. It will be shown that the shape of hard-core particles is of crucial importance for the stability of the phases. Both static and dynamic properties of the systems are obtained by means of computer simulation.

### 1. Introduction

Liquid crystals are partially ordered fluids [1]. The simplest is the *nematic* phase in which the molecules are translationally disordered but the molecular orientations are not distributed randomly. Rather, the molecular axes tend to align parallel to some, otherwise arbitrary, direction. This alignment axis is usually referred to as the nematic director  $n$ . A quantitative measure for the degree of alignment is the nematic order parameter  $s$ . For axially symmetric molecules,  $S$  is defined as  $\langle P_2(\cos \theta) \rangle$ , where  $\theta$  is the angle between the molecular symmetry axis and the nematic director. In the isotropic fluid phase,  $S = 0$ . In a perfectly aligned nematic  $S = 1$ . The phase transition from isotropic liquid to nematic liquid crystal is weakly first order. By 'weakly first order' I mean that the transition, although first order, is preceded by strong precursor effects as is usually the case in the vicinity of continuous phase transitions. The transition from both the nematic and the isotropic phases to the solid is a normal first order transition. Most isotropic molecular liquids freeze as the temperature is lowered. But only some form liquid crystals. An obvious question is: what determines whether a molecular liquid forms a liquid crystal before it freezes?

All molecules that form nematics are non-

spherical, but the converse is not true. In other words, a certain degree of non-sphericity is a necessary, but not a sufficient condition for liquid crystal formation. Several other factors also play a role in determining the relative stability of the nematic phase. For instance, attractive intermolecular interactions due to dispersion forces also tend to favor parallel alignment of the molecules. There are a number of models that attribute the orientational ordering in liquid crystals to the effect of dispersion forces [2,3], including the original mean-field model due to Maier and Saupe. Although these models yield fair estimates for a number of properties of nematic liquid crystals, they cannot be used to explain the stability of the nematic phase with respect to the solid. It is quite conceivable that in some cases dispersion forces would stabilize the solid more than the nematic. Another factor that influences the stability of liquid crystals is the presence of flexible tails (often alkane or alkoxy chains) connected to the 'rigid' core of the nematogen. That flexible chains are indeed important for the stability of liquid crystals follows from the experimental observation that essentially all liquid crystal forming molecules ('mesogens') have them [4]. If the tail is shortened too much the liquid freezes without ever becoming nematic. A model that takes into account the effect of the flexible tails on the relative stability of isotropic, nematic and smectic phases was developed by Dowell and Martire [5]. But, to my knowledge, a quantitative comparison with the solid has not been made.

For someone who is familiar with the theory of

\* Part of the material reviewed in this article appeared in the January 1986 issue of *Molecular Physics*.

<sup>1</sup> Present address: FOM Institute for Atomic and Molecular Physics, P.O. Box 41883, 1009 DB Amsterdam, The Netherlands.

simple liquids it is natural to assume that, of the factors mentioned above, the hard-core repulsions are most important. Of course, the 'natural' assumption is not necessarily the correct one, and the only way to find out is to try. Trying in this case means computer simulation. However, before we turn to the computer simulations let me briefly sketch what we know from experiment about the relation between molecular shape and the tendency to form liquid crystals [6]. First of all, we know that liquid crystals can consist of both rod-like and plate-like molecules. Most rod-like mesogens have length-to-breadth ratios between 3 and 4 (it should be noted, however, that this ratio is a rather fuzzy concept for molecules with flexible tails). What we know at present about disc-like mesogens (see e.g. ref. [7]) suggests that these molecules are even less spherical. It is not straightforward to tell from experiment how the isotropic-nematic and the nematic-solid transitions depend on the shape of the repulsive core of the molecules. The problem is that although a wealth of data on the phase transitions of molecules with different shapes are available, we do not know how to disentangle the effects of molecular shape, dispersion forces and flexible tails.

Next, let us consider what we know from theory and earlier computer simulations. For hard spheres we do know the melting point from the computer simulations of Hoover and Ree [8]. But these simulations do not tell us what will happen to the melting point as the molecular shape changes from spherical to rod-like or plate-like. The Onsager theory [9] predicts that thin spherocylinders with length  $L$  and diameter  $D$  undergo a transition from the isotropic to the nematic phase at a density of order  $1/L^2D$ . At this density the fraction of the volume occupied by the spherocylinders is still vanishingly small (order  $D/L$ ). The same holds for infinitely thin hard platelets [10]. For neither of these model systems do we know the melting point.

## 2. Computer simulations of nematogens

To find out about the phase behavior of non-spherical hard core molecules, we performed

Monte Carlo simulations on a simple model system, viz. hard ellipsoids of revolution. The shape of such a spheroid is characterized by a single parameter,  $x$ , the ratio of the length of the major axis ( $2a$ ) to the minor axis ( $2b$ ):  $x = a/b$ . Special cases are:  $x = 1$  (hard spheres),  $x \rightarrow \infty$  (hard needles [9]) and  $x \rightarrow 0$  (hard platelets [10]). Technical details of the Monte Carlo simulations have been published elsewhere [11]. Here I shall concentrate on the results. We carried out constant pressure Monte Carlo simulations for hard spheroids with 8 different length-to-breadth ratios  $x$  in the range between  $1/3$  (oblate) and  $3$  (prolate). Typical examples of the resulting isotherms are shown in fig. 1. The isotherms shown in fig. 1 consist of two branches: a low density branch corresponding to the isotropic fluid phase, and a high density solid branch. Direct coexistence between solid and liquid cannot be observed in these small systems ( $\mathcal{O}(10^2)$  particles) with periodic boundary conditions. In fig. 1 no nematic branch is observed because the molecules are not sufficiently anisometric. What is striking about fig. 1 is the strong resemblance between isotherms for particles with reciprocal length-to-breadth ratios. Actually, we find such almost symmetric behavior for all spheroids that we studied. A more quantitative measure of this symmetry is shown in fig. 2. In this figure the percentual difference of the pressure of oblate and prolate ellipsoids is plotted as a function of density. At low densities this difference goes to zero. This is understandable because, in the present units, the second virial coefficients of spheroids with inverse length-to-breadth ratio's are equal [12]. However, no such symmetry holds for the higher virial coefficients. In particular, Onsager has argued that in the limit  $x \rightarrow \infty$ ,  $B_3/B_2^2 \rightarrow 0$ . But in the limit  $x \rightarrow 0$ , this same ratio tends to a finite value of 0.4447 [10]. The approximate oblate-prolate symmetry at higher densities shown in fig. 2, is therefore not exact, which makes it all the more surprising.

### 2.1. Orientational order

Let us next look for orientationally ordered phases. Fig. 3 shows the equation of state of spheroids with  $a/b > 2.75$  and  $a/b < (1/2.75)$  at

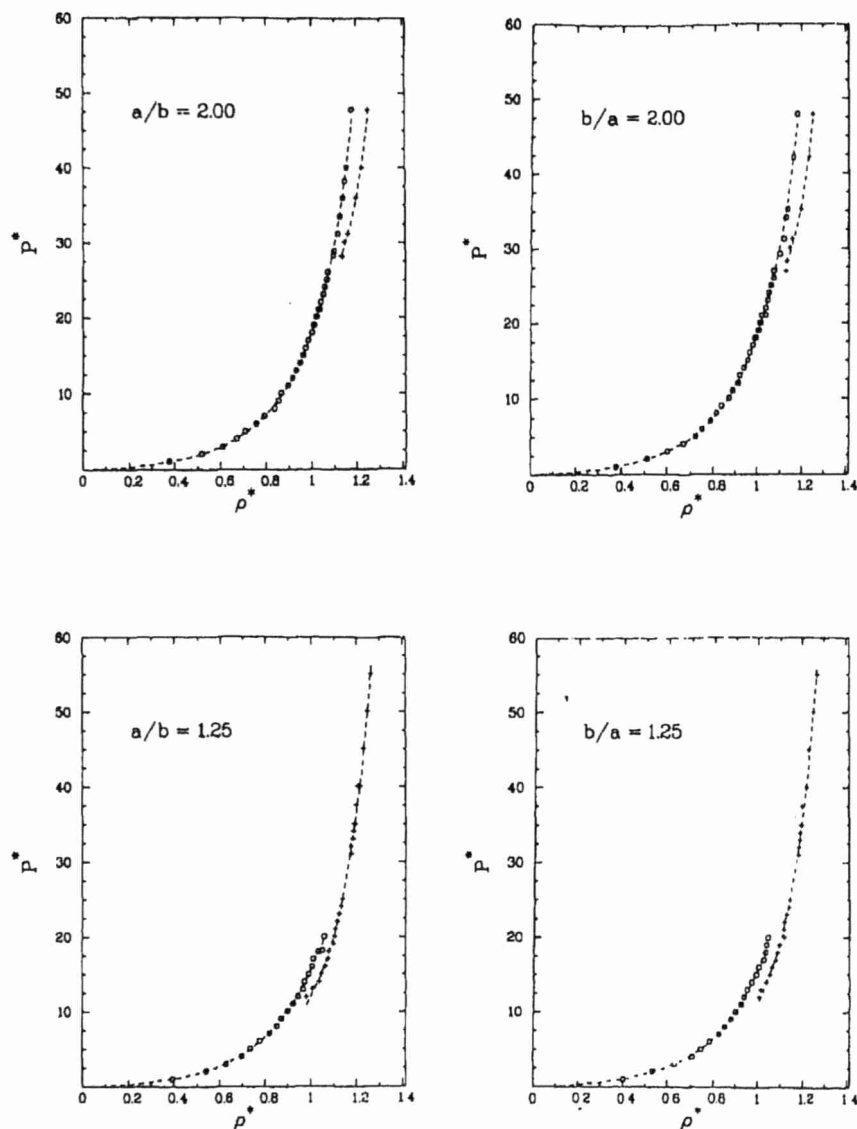


Fig. 1. Equation of state of hard ellipsoids of revolution with length-to-breadth ratios  $x = 2, 1.25, 0.8$  and  $0.5$ . The pressure is in units  $kT/8ab^2$ , the density in units  $(8ab^2)^{-1}$ . Open circles: (isotropic) fluid branch, pluses: solid branch.

densities around the melting point. Between the solid and the isotropic fluid branch we observe a third branch which corresponds, as we shall show, to a nematic liquid crystal. There are several methods to detect a nematic phase in a computer simulation. A particularly simple technique is to monitor the behaviour of the pair distribution

function, in particular the part that depends on the relative orientation of molecules at a distance  $r$ . A useful measure of the degree of orientational order is given by  $g_2(r)$ , defined as the average value of  $P_2(\cos \theta)$  for molecules with a center of mass distance  $r$ ;  $\theta$  is the angle between the molecular axes. In the isotropic phase  $g_2(r)$  decays to

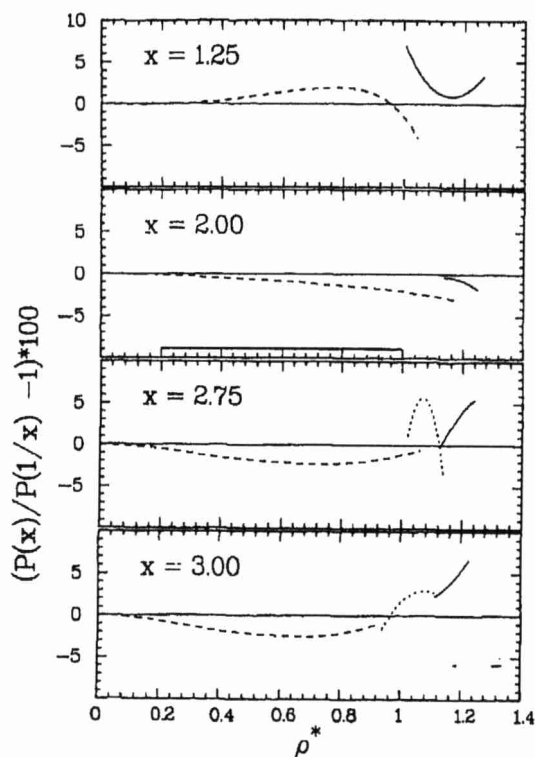


Fig. 2. Deviations from perfect symmetry between the equations of state of hard ellipsoids of revolution with inverse length-to-breadth ratios. The ordinate shows the percentual difference between the pressure of a fluid of hard ellipsoids with  $a/b = x$  and  $b/a = x$ , both at density  $\rho$ . Dashed curve: isotropic branch, dotted curve: nematic branch, drawn curve: solid branch. The curves shown in this figure were obtained from fits to the equation of state data (see ref. [11]).

zero within a few molecular diameters. In contrast, in the nematic phase  $g_2(r)$  becomes long ranged. As  $r \rightarrow \infty$ ,  $g_2(r) \rightarrow S^2$  is the nematic order parameter. Of course, in a computer simulation we can never measure correlations at distances greater than half the periodic box diameter,  $L$ . But, as fig. 4 shows, even the behaviour of  $g_2$  at  $r = L/2$  is a useful indicator of the onset of orientational order. Fig. 4 illustrates another important feature of the isotropic–nematic transition in a system of prolate hard ellipsoids, namely the fact that it exhibits hysteresis. Hysteresis is usually observed at first order phase transitions. However,

the isotropic–nematic transition is only weakly first order and, as a consequence, hysteresis may be suppressed by fluctuations. For oblate ellipsoids, hysteresis appears to be weaker than for prolate ellipsoids. Why this should be so is not clear at present.

## 2.2. Phase diagram

Using the methods described in ref. [11], the free energy of all phases of the system of hard ellipsoids was computed and the phase transitions located. The resulting ‘phase diagram’ is shown in fig. 5. In this figure the molecular shape varies from left to right from extremely oblate ellipsoids (‘platelets’), through spheres to extremely prolate ellipsoids (‘needles’). The ordinate measures the density which, in the present units, varies between 0 and  $\sqrt{2}$  (regular close packing). Four distinct phases can be identified, the isotropic fluid (I), nematic fluid (N), orientationally ordered solid (S) and orientationally disordered (plastic) solid (PS). The shaded areas represent two-phase coexistence regions. Several aspects of fig. 5 are worth noting. First of all the phase diagram has a high degree of symmetry under the interchange of oblate and prolate ellipsoids. As in fig. 2 above, this symmetry is not perfect. The physical reason for this near symmetry is not understood at present. Fig. 5 also provides us with an answer to the old question: what is the minimum non-sphericity needed to form a stable nematic phase? Clearly, for ellipsoids with axial ratios approximately between 1/2.5 and 2.5, no stable nematic phase is possible. As a bonus, we obtain an estimate of the range of stability of the orientationally disordered solid phase (approximately between  $a/b = 1/1.5$  and  $a/b = 1.5$ ) although in this case the boundaries are less well determined.

Now that we know the range of stability of the nematic phase in this model system, let us look in more detail at the physical consequences of the onset of orientational ordering. In the isotropic phase, the presence of a nematic is betrayed by an increase in the amplitude of collective orientational fluctuations. Below we shall illustrate what computer simulation can tell us about such pre-transitional phenomena.

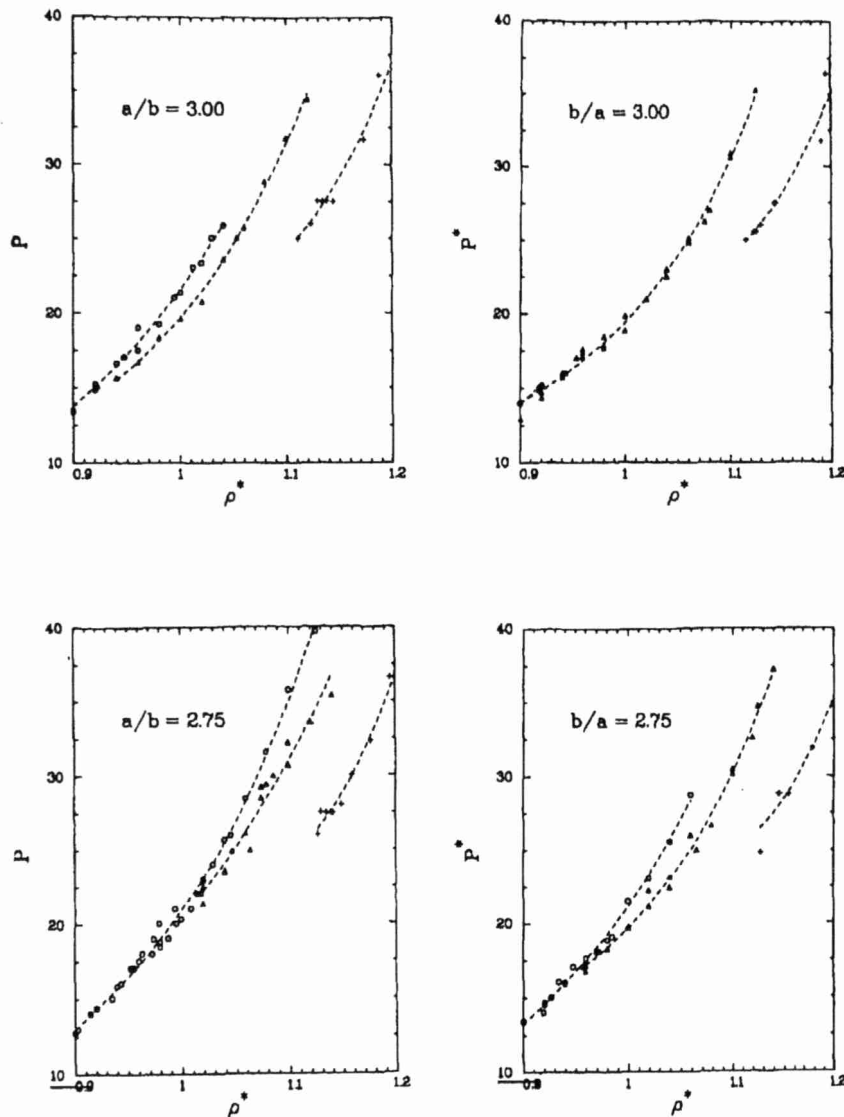


Fig. 3. Equation of state of hard ellipsoids of revolution with length-to-breadth ratios 3, 2.75, 1/2.75 and 1/3, in the density range where a nematic branch is observed. Open circles: (isotropic) fluid branch, triangles: nematic branch, plusses: solid branch. The units are as in fig. 1.

### 2.3. Orientational precursor effects

At the transition to the nematic phase spontaneous ordering of the molecular orientations takes place. Although this macroscopic ordering occurs at a well defined state point, strong pretransitional

fluctuations may be observed in the isotropic phase as the transition to the nematic phase is approached. This results, among other things, in enhanced depolarized light scattering. To a first approximation, the intensity of depolarized light scattering,  $I_d$ , is proportional to the average trace

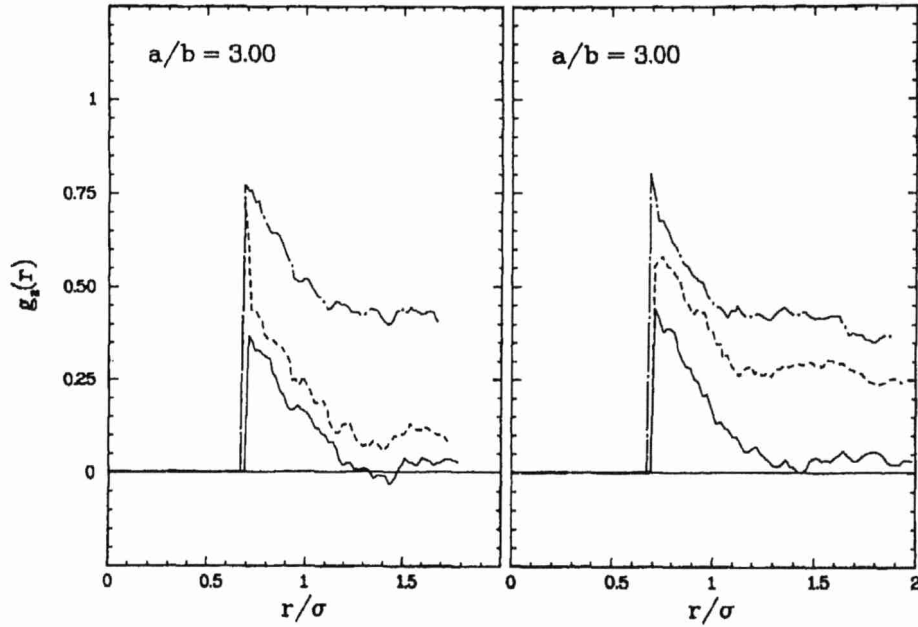


Fig. 4. Example of the behaviour of the orientational correlation function  $g_2(r) = \langle P_2(u(0) \cdot u(r)) \rangle$  of hard ellipsoids of revolution with  $a/b = 3$  in the vicinity of the I-N transition. Densities:  $\rho/\rho_0 = 0.65$  (drawn curve),  $\rho/\rho_0 = 0.707$  (dashed curve), and  $\rho/\rho_0 = 0.778$  (dash-dot). The left-hand side shows the behaviour of  $g_2(r)$  on compression. The right-hand side shows the corresponding results for expansion.

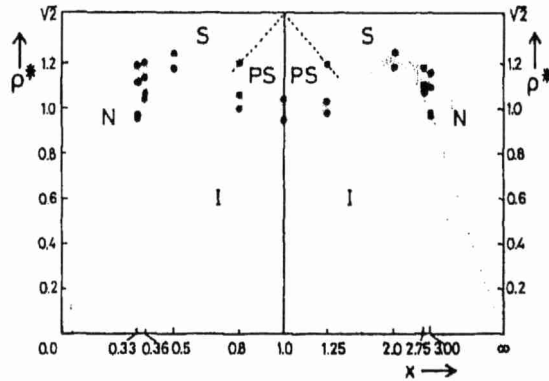


Fig. 5. 'Phase diagram' of hard ellipsoids of revolution. Vertical axis: density in units  $(8ab^2)^{-1}$ . Horizontal axis: Length-to-breadth ratio,  $x$ . The shaded areas correspond to two-phase regions. The dots are the computed coexistence points. The points for  $x = 1$  were taken from ref. [8]. The following phases can be distinguished: isotropic fluid (I), nematic liquid crystal (N), orientationally ordered solid (S) and plastic solid (PS).

of the square of the collective orientational tensor  $Q$ :

$$I_d \sim \langle Q_{\alpha\beta} Q_{\beta\alpha} \rangle, \quad (1)$$

where  $Q$  is defined as:

$$Q_{\alpha\beta} = \frac{1}{N} \sum_i \{ 3u_\alpha^i u_\beta^i - \delta_{\alpha\beta} \} / 2, \quad (2)$$

Landau theory predicts that, to a first approximation:

$$I_d \sim (\rho^* - \rho)^{-1}, \quad (3)$$

where  $\rho^*$  is the density at which the isotropic phase becomes absolutely unstable.  $\langle Q_{\alpha\beta} Q_{\beta\alpha} \rangle$  in eq. (1) is a measure for the correlation of the orientation of different molecules. It is easy to show that  $\langle Q_{\alpha\beta} Q_{\beta\alpha} \rangle = 1.5(1 + g_2)/N$ , where  $g_2$  is the static orientational correlation factor, defined as:

$$g_2 = \sum_{i \neq j} P_2(u_i \cdot u_j). \quad (4)$$

The proximity of the isotropic–nematic transition influences not just the static orientational properties of the fluid but also the rotational dynamics. In particular, the relaxation time  $\tau_2^c$  of the collective orientation fluctuations diverges as the I–N transition is approached. The relation between the divergence of  $g_2$  and  $\tau_2^c$  is of particular interest. Using Mori theory, Keyes and Kivelson [13] derived the following expression relating  $g_2$  to  $\tau_2^c$  [14]:

$$\tau_2^s/\tau_2^c = (i + j_2)/(1 + g_2). \quad (5)$$

Here  $\tau_2^s$  is the single-particle correlation time and  $j_2$  is the dynamic orientational correlation factor. The latter quantity can be expressed in terms of memory functions, but has no simple physical interpretation. A direct experimental determination of  $(1 + g_2)$  and  $\tau_2^s/\tau_2^c$  is complicated by the fact that in real liquids part of the depolarized light scattering intensity is interaction induced. It is not trivial to separate out the purely orientational contribution to the scattering intensity [15]. As a consequence, there is a scarcity of reliable data from which  $j_2$  can be determined. The available information (see e.g. ref. [16]) suggests that  $j_2$  is small compared to 1, and it is common practice among light scatterers to assume that  $j_2 = 0$ .

Numerical simulation offers a unique possibility to study the static and dynamic precursor effects to the I–N transition in simple model systems. As an example, we consider the pretransitional behaviour in a system of prolate hard ellipsoids with  $a/b = 3$  [17]. From the Monte Carlo simulations mentioned above, we know that this system has a transition from the isotropic to the nematic phase at 70% of the density of regular close packing. For comparison, we also studied the orientational dynamics of hard ellipsoids with  $a/b = 2$ . The latter system has no stable nematic phase and hence we should expect it to behave rather differently from the more anisometric  $a/b = 3$  system. Fig. 6 shows typical examples of  $C_1(t) \equiv \langle P_1(u(0) \cdot u(t)) \rangle$  and  $C_2(t) \equiv \langle P_2(u(0) \cdot u(t)) \rangle$ , the correlation functions of the first and second Legendre polynomials of the molecular orientation vectors. Both  $C_1(t)$  and  $C_2(t)$  are single-particle correlation functions [18]. In the rotational diffusion limit, the ratio of the relaxa-

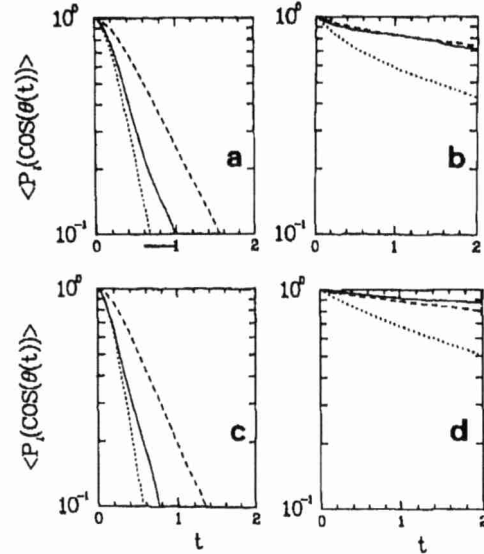


Fig. 6. Density and shape dependence of single-particle and collective orientational correlation function for hard ellipsoids of revolution. (a)  $a/b = 2$ ,  $\rho/\rho_0 = 0.5$ ; (b)  $a/b = 2$ ,  $\rho/\rho_0 = 0.8$ ; (c)  $a/b = 3$ ,  $\rho/\rho_0 = 0.3$ ; (d)  $a/b = 3$ ,  $\rho/\rho_0 = 0.7$ . Single-particle first-rank orientational correlation function  $C_1^s(t) = \langle P_1(u(0) \cdot u(t)) \rangle$ , (—). Single-particle second-rank orientational correlation function:  $C_2^s(t) = \langle P_2(u(0) \cdot u(t)) \rangle$ , (---). Collective second-rank orientational correlation function,  $C_2^c(t) = \sum_j \langle P_2(u_i(0) \cdot u_j(t)) \rangle$  (····). The single-particle orientational variable has been made orthogonal to the collective one by projection. Note that at high densities the decay of  $C_2^c(t)$  becomes much slower than that of  $C_2^s(t)$ .

tion times of  $C_1(t)$  and  $C_2(t)$ ,  $\tau_2^1/\tau_2^s$  equals 3. We find that this behaviour well obeyed at not too low densities. Both single particle relaxation times grow as the density is increased. This is simply a consequence of the rapid increase of the viscosity as the density of the fluid is raised, and the effect is observed for both shapes of ellipsoids. The density dependence of the collective orientational correlation function,  $C_2^c(t) \equiv \sum_j \langle P_2(u_i(0) \cdot u_j(t)) \rangle$  is more interesting. At low densities, the decay of  $C_2^c(t)$  closely follows that of  $C_2^s(t)$ , as can be seen from fig. 6. However, as the density is increased, the decay of the collective orientational correlation function becomes much slower than the corresponding single-particle one. Hence, cooperative effects in the rotational dynamics become important at high densities, both for the  $a/b = 2$  and for  $a/b = 3$  case. Fig. 7 shows the density depen-



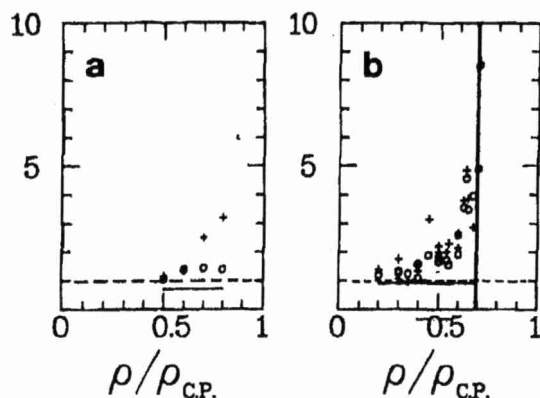


Fig. 7. Density dependence of the ratio  $\tau_2^c/\tau_2^s$  (plusses), for hard ellipsoids of revolution with  $a/b=2$  (a) and  $a/b=3$  (b). Also shown is the behaviour of the static orientational correlation factor ( $1+g_2$ ) (open circles). The best estimate for the dynamic orientational correlation factor ( $1+j_2$ ) is shown as a horizontal line. In (b) the isotropic-nematic coexistence region is bordered by parallel vertical lines.

dence of the ratio  $\tau_2^c/\tau_2^s$  for both shapes of ellipsoids. In the same figure we have also plotted the corresponding values of  $(1+g_2)$ . The difference in the behaviour of the  $a/b=3$  and  $a/b=2$  ellipsoids is immediately apparent. For  $a/b=2$  there is evidence for some cooperative behaviour, but even at the freezing density (at 84% of close packing), there is no sign of diverging fluctuations or critical slowing down. In contrast, the results for  $a/b=3$  clearly show pretransitional effects. Both  $\tau_2^c/\tau_2^s$  and  $(1+g_2)$  appear to diverge as the transition to the nematic phase is approached. If the dynamic orientational correlation factor  $j_2$  vanishes, then the data points for  $\tau_2^c/\tau_2^s$  and  $(1+g_2)$  should superimpose. The simulations suggest that  $j_2$  is small and negative, but on this point the simulations appear inconclusive.

### 3. Beyond nematics

In the previous sections we have shown that sufficiently anisometric hard ellipsoids of revolution can form thermodynamically stable nematic phases. Naturally, the question arises whether other liquid-crystalline phases, for instance

smectics, can also be found in hard core systems. This is not obvious a priori. In fact, to my knowledge, most textbooks on liquid crystals do not even seriously consider this possibility (see however, ref. [19]). Even more than in the case of nematics, dispersion forces [20] and the effects of flexible tails [5] are held responsible for the formation of smectic phases. Although we do not contest that these factors must have a pronounced effect on the stability of smectics, the question is whether they are essential.

In order to explore the possibility of smectic order in rigid hard-core systems, we carried out Monte Carlo and molecular dynamics simulations on model systems consisting of parallel spherocylinders with diameter  $D$  and length  $L$  (i.e. the hemispherical caps were separated by a straight cylindrical segment of length  $L$ ) [21]. As the particles in this system are always perfectly aligned, the low-density phase is a "nematic" fluid. The parallel spherocylinder fluid can be thought of as a model for a fluid of rod-like particles in a strong magnetic field. We know that the corresponding hard-ellipsoid model will not exhibit smectic order. Simulations were carried out for systems of parallel spherocylinders with  $L/D$  ratios of 0.25, 0.5, 1, 2, 3 and 5. The well-known case  $L/D=0$  (i.e. hard spheres) was also studied, as a check. We computed the absolute free energies of both the fluid and the solid phases. Combining the free energy and equation of state data, we can determine the dependence of the melting point of the spherocylinder crystal on  $L/D$ . Having determined the limits of thermodynamic stability of the solid phase, the next step is to look for possible fluid-fluid phase transitions. No discontinuities or Van der Waals loops are observed in the fluid branch of the equation of state [21], but for the larger  $L/D$  ratios we observe a rather sudden change in the compressibility at densities between 40% and 60% of close packing. Snapshots of typical molecular configurations both below and above this 'cusp' in the equation of state (fig. 8) show a dramatic change in the structure of the fluid. At low densities, the fluid is translationally disordered. Then, at a higher density (but well before the freezing point), the fluid orders into parallel layers, but there is no order within the layers. In



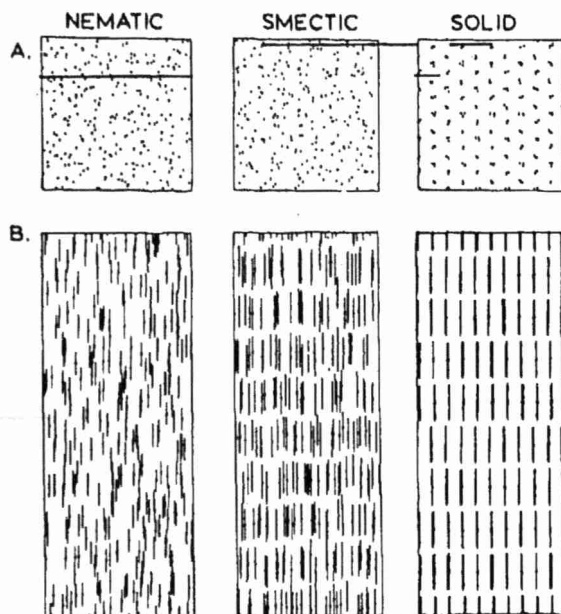


Fig. 8. Snapshots of typical molecular configurations of a system of 270 parallel hard spherocylinders with  $L/D = 5$ . Left: nematic phase ( $\rho/\rho_0 = 0.24$ ). Middle: smectic phase ( $\rho/\rho_0 = 0.62$ ). Right: solid phase ( $\rho/\rho_0 = 0.89$ ). The upper figures (A) show a projection in the plane perpendicular to the molecular axes, the lower figures (B) show a projection in a plane through the molecular axes. For the sake of clarity, the spherocylinders are indicated by a line segment of length  $L$ .

other words, the parallel spherocylinder form a smectic-A phase [22]. For comparison, the crystalline phase, at still a higher density, is also shown. In the latter case there is clearly translational order within the layers.

A more quantitative method to locate the transition to the smectic phase is to study the static and dynamic behaviour of the longitudinal component of the intermediate scattering function  $F(k_z, t)$ , defined as:

$$F(k_z, t) = \langle \rho(k_z, 0) \rho(-k_z, t) \rangle, \quad (6)$$

where  $\rho(k_z, t)$  is the instantaneous amplitude of a longitudinal density fluctuation with wavevector  $k_z$ .  $F(k_z, t=0)$  is the longitudinal part of the static structure factor,  $S(k_z)$ , which determines, for instance, the X-ray scattering intensity. As the smectic phase is approached from lower densities,

there will be smectic precursor fluctuations. These will show up as peaks in  $S(k_z)$ , for values  $k_z$  equal to (multiples of)  $2\pi/d$ , where  $d$  is the spacing of the incipient smectic layers. If the transition to the smectic phase is continuous, the peaks in  $S(k_z)$  will diverge at the transition. Incipient smectic ordering leads to a critical slowing down of the correlation function  $F(k_z, t)$  at  $k_z = k_z(\text{max})$ . As can be seen from fig. 9, the decay rate of  $F(k_z(\text{max}), t)$  first increases as the density is raised, because the fluid is less compressible at higher densities. But beyond a certain density the decay rate drops precipitously to zero. This provides us with an estimate for the nematic-smectic transition density. For comparison, fig. 9 also shows an example of a fluid which does not become smectic ( $L/D = 0.25$ ). In this case the decay rate of  $F(k_z(\text{max}), t)$  depends only weakly on density.

Combining the information about the smectic order parameter fluctuations with the data on the melting transition, we can construct a 'phase diagram' of hard parallel spherocylinders (fig. 10). This phase diagram shows the regions of stability of the nematic, smectic and solid phases as a function of  $L/D$ . For  $L/D \geq 0.5$ , a smectic phase is found between the crystalline solid and the 'nematic' fluid. As the non-sphericity of the particles is increased, the smectic range initially grows

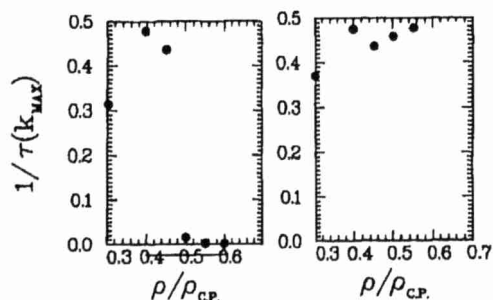


Fig. 9. Relaxation rate of the longitudinal density fluctuations with a wavevector corresponding to the first maximum in  $S(k_z)$ . Left figure: parallel spherocylinders with  $L/D = 0.25$ , this system does not form a stable smectic. The figure shows no evidence for critical slowing down. Right-hand figure: parallel spherocylinders with  $L/D = 1$ . This system does form a smectic. As the transition is approached, the decay rate of the smectic precursor fluctuations drops dramatically.

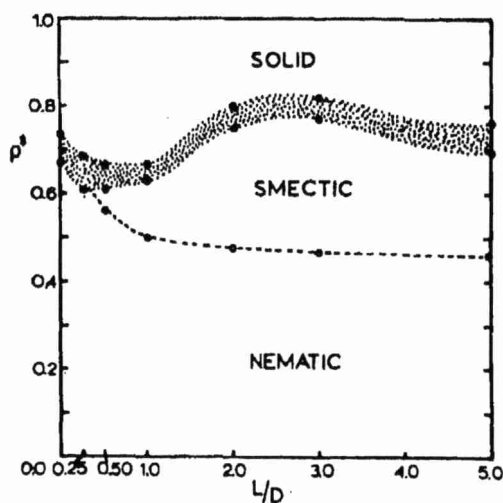


Fig. 10. Schematic 'phase diagram' of hard parallel spherocylinders, as a function of length-to-width ratio  $L/D$ . The shaded area corresponds to the fluid-solid two-phase region. Black circles: densities of the coexisting fluid and solid phase. Open circles: densities at which smectic ordering sets in. The dashed line indicates the estimated nematic-smectic phase boundary.

and then saturates [23]. It should be stressed that this phase diagram pertains to a system of parallel spherocylinders. The effect of the orientational degrees of freedom on the phase diagram is currently under investigation [24].

#### 4. Conclusions

In this paper I have tried to demonstrate that model systems consisting of non-spherical hard-core particles have a surprisingly rich phase diagram. In the case of hard ellipsoids, we found that the stability of the nematic phase is simply related to the degree of non-sphericity of the molecules. Moreover, even though parallel ellipsoidal particles cannot form stable smectics, parallel spherocylinders can. This result is quite unexpected because of the apparent similarity of long spherocylinders and needle-like ellipsoids.

In addition I have shown how a number of the physically interesting static and dynamic properties of liquid-crystal-forming fluids can be studied by computer simulation. The interest of such

calculations lies not so much in the possibility to reproduce the behaviour of real liquid crystals (although it is encouraging to find qualitative agreement). The use of these, and future, calculations is that they can be used to test approximate theoretical expressions for a wide variety of equilibrium and transport properties of molecular liquids and liquid crystals.

#### Acknowledgements

I gratefully acknowledge many stimulating discussions with Bela Mulder, Henk Lekkerkerker and Alain Stroobants. The molecular dynamics calculations described in this paper employed a vectorized code for non-spherical hard-core molecules which was developed in collaboration with Mike Allen.

#### References

- [1] P.G. de Gennes, *Physics of Liquid Crystals* (Oxford Univ. Press, London, 1974).
- [2] W. Maier and A. Saupe, *Z. Naturf.* A13 (1958) 564.
- [3] W.M. Gelbart and A. Gelbart, *Mol. Phys.* 33 (1977) 1387.
- [4] This holds for *thermotropic* liquid crystals. For *lyotropic* liquid crystals flexible tails play no role, although here the flexibility of the particle as a whole may be important, see: T. Odijk, *Polymer Commun.* 26 (1985) 197.
- [5] F. Dowell and D.E. Martire, *J. Chem. Phys.* 68 (1978) 1088, 1094, 69 (1978) 2322.  
F. Dowell, *Phys. Rev. A* 28 (1983) 3526.
- [6] See e.g. G.W. Gray, in: *The Molecular Physics of Liquid Crystals*, eds. G.R. Luckhurst and G.W. Gray (Academic Press, London, 1979) p. 1, 263.
- [7] C. Destrad, P. Fouchet, H. Gasparoux, N.H. Tinh, A.M. Levelut and J. Malthete, *Mol. Cryst. Liq. Cryst.* 106 (1984) 121.
- [8] W.G. Hoover and F.H. Ree, *J. Chem. Phys.* 49 (1968) 3609.
- [9] L. Onsager, *Ann. N.Y. Acad. Sci.* 51 (1949) 627.
- [10] R. Eppenga and D. Frenkel, *Mol. Phys.* 52 (1984) 1303.
- [11] D. Frenkel and B.M. Mulder, *Mol. Phys.* 55 (1985) 1171.
- [12] A. Isihara, *J. Chem. Phys.* 19 (1956) 1142.
- [13] T. Keyes and D. Kivelson, *J. Chem. Phys.* 56 (1974) 1057.
- [14] Unfortunately, there is some confusion in the literature about the notation used for the static and dynamic correlation factors ( $1 + g_2$ ) and  $(1 + j_2)$ . Here we have chosen a definition of  $g_2$  and  $j_2$  such that both quantities vanish in the absence of correlations.

- [15] For a discussion, see: D. Kivelson and P.A. Madden, *Ann. Rev. Phys. Chem.* 31 (1980) 523.
- [16] G.R. Alms, T.D. Gierke and W.H. Flygare, *J. Chem. Phys.* 61 (1974) 4083.
- [17] T.D. Gierke and W.H. Flygare, *J. Chem. Phys.* 61 (1974) 2231.
- [18] M.P. Allen and D. Frenkel, submitted for publication.
- [19] Actually, the correlation functions shown are the orthogonalized single-particle and collective orientational correlation functions.
- [20] M. Hosino, H. Nakano and H. Kimura, *J. Phys. Soc. Japan* 46 (1979) 1709.
- [21] W.L. McMillan, *Phys. Rev. A* 4 (1971) 1238.
- [22] A. Stroobants, H.N.W. Lekkerkerker and D. Frenkel, *Phys. Rev. Lett.* 57 (1986) 1452.
- [23] We also checked for long-range bond-orientational order within the layers, but did not find any. Hence the fluid is not a hexatic-B phase.
- [24] More recent evidence indicates that the phase diagram is even richer than shown in the figure, A. Stroobants et al., to be published.
- [25] D. Frenkel, *J. Phys. Chem.* (in press).